- Technical Paper -

EFFECTS OF PRESTRESSING METHOD ON FLEXURAL PERFORMANCE OF PCa BEAMS

Zheming HUANG[*1], Kazumasa OKUBO[*2] and Junichiro NIWA[*3]

ABSTRACT

This paper proposes an engineering attempt to apply prestressing force at the interface in a PCa beam by using non-abutment pretensioning prestressing method (NAPP method). Static cyclic loading tests considering the existence of interface and prestressing force were conducted on three specimens. The results showed that prestressing method can effectively reduce the deflection and interface opening in PCa beams and improve the ductility and cracking resistance. Besides, the yielding load and ultimate flexural capacity of PCa beams were not affected by the interface and the prestressing force.

Keywords: prestressing method, flexural performance, PCa beam, joint connection, interface

1. INTRODUCTION

Nowadays precast (PCa) concrete structure has been adopted more and more widely in construction industry. In PCa structures, the key issue is how to connect PCa members. One general method is to use the mortar grouted sleeve. This is a representative of mechanical joints consisting of steel sleeve with infilled high strength mortar in which reinforcing bars of two PCa segments are spliced together. Although the previous research [1] indicated that the strength of joint in PCa beams can be ensured by using mortar grouted sleeves, it is also reported [2] that the interface opening values between PCa segments were significantly larger than the maximum crack widths. With wide opening interface, harmful substances may easily penetrate into the concrete and lead to problems such as corrosion of reinforcement, causing negative impacts on the long-term structural performance. Therefore, effective methods to reduce the interface opening between PCa segments need to be proposed immediately to ensure the durability of PCa structures.

This study proposed an engineering attempt to apply prestressing force at the interface in a PCa beam by using non-abutment pretensioning prestressing method (NAPP method), in which two PCa segments are connected by a NAPP unit. NAPP, abbreviation for non-abutment pretensioning prestressing, is a method to introduce prestressing force into a concrete member by releasing a pretensioned hollow steel bar. This process is illustrated in Fig. 1. The NAPP unit was manufactured in the factory and stayed in a pretensioned state while it is transported to the construction site. When it is released, the pretensioned hollow steel bar will shrink naturally and transfer compressive stress to concrete by the bonding between steel bar and concrete or mortar. In this way the existing concrete member and strengthening concrete member are tightly clamped together [3].

In this study, to investigate the effectiveness of the prestressing method in PCa structures, cyclic loading tests were conducted on two PCa beams and one monolithic beam without interface as a reference. Mortar grouted sleeves were used to connect the steel bars of two PCa segments and the parameter was the prestressing force at the bottom fiber of concrete at the interface. The effectiveness of prestressing force in PCa beams and flexural performance of the specimens were discussed in this paper.

2. TEST PROGRAMS

2.1 Test Specimens and Materials

Specimens in this study are summarized in Table 1 and their dimensions and reinforcement arrangement are shown in Fig. 2. Specimen N-P0 and N-P1.0 consisted of two PCa segments cast separately with the length of 1800 mm, while N-Ref was cast as a whole with the length of 3600 mm. All specimens shared same dimensions and reinforcement arrangement except that there was no mortar interface in the reference beam N-Ref. All the longitudinal reinforcements including those in N-Ref used in this study were connected by mortar grouted sleeves. Section height of the specimens was 465 mm with effective depth of 418mm and the section width was 300 mm. Two typical sections A-A' and B-B' are also shown in Fig. 2, where a 450 mm-long, 150 mm-wide and 220 mm-high perforated hole was created for releasing the NAPP unit shown in section A-A' and a 560 mm-long sheath was created to insert the NAPP unit. The sheath was grouted after two PCa segments were connected and the perforated hole was grouted after the releasing of NAPP unit. The location of NAPP unit and

*1 Graduate student, Dept. of Civil and Environmental Engineering, Tokyo Institute of Technology, JCI Student Member

*2 Commissioned researcher, Dept. of Civil and Environmental Engineering, Tokyo Institute of Technology, JCI Member

*3 Prof., Dept. of Civil and Environmental Engineering, Tokyo Institute of Technology, Dr. E., JCI member

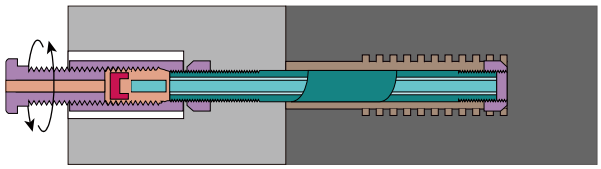

(a) Releasing the NAPP unit

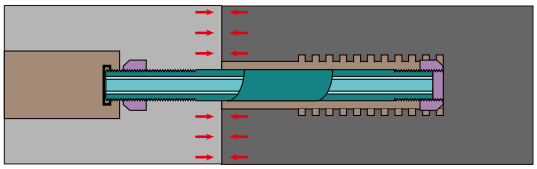

(b) After releasing

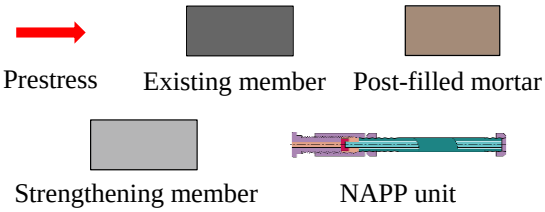

Fig. 1 Principle of NAPP method

the anchoring length, which was 500 mm both in concrete and mortar, were determined according to the Construction and Design Manual of NAPP Anchoring Method [3].

As shown in Table 1, all specimens were cast in concrete with design cylinder compressive strength of 40 N/mm^2 and the compressive strengths of mortar used in the perforated hole as well as the interface and mortar grouted sleeves were 60 N/mm^2 and 120 N/mm^2, respectively. Specimen N-P1.0 corresponds to that the

Table 1 Specimen summary

Specimen	Joint	f'_{cd} (N/mm^2)	σ_{cld} (N/mm^2)
N-Ref	-	40	0
N-P0	20-mm thick mortar interface		
N-P1.0			2.74

f'_{cd}: design cylinder compressive strength of concrete, σ_{cld}: design value of compressive stress at the bottom fiber of concrete at the interface

design compressive stress brought by prestressing at the bottom fiber of concrete at the interface was one times of concrete tensile strength. Here concrete tensile strength was derived from Eq. 1 suggested by Japan Society of Civil Engineers Standard Specifications for Design and Construction of Concrete Structures (JSCE Standard Specification) [4], which is

$$f_{tk} = 0.23 f'^{2/3}_{ck} \quad (1)$$

where f_{tk} is the characteristic tensile strength of concrete and f'_{ck} is the characteristic compressive strength.

2.2 Loading Method and Instrumentation

All specimens were designed to fail in flexure and four-point bending tests with pure bending region of 600 mm long were conducted as illustrated in Fig. 2. Simply-supported condition was created by inserting teflon sheets with grease between the supports and specimens. Concrete strain gauges were attached on the side surface of the specimens at the interface to measure the strain in

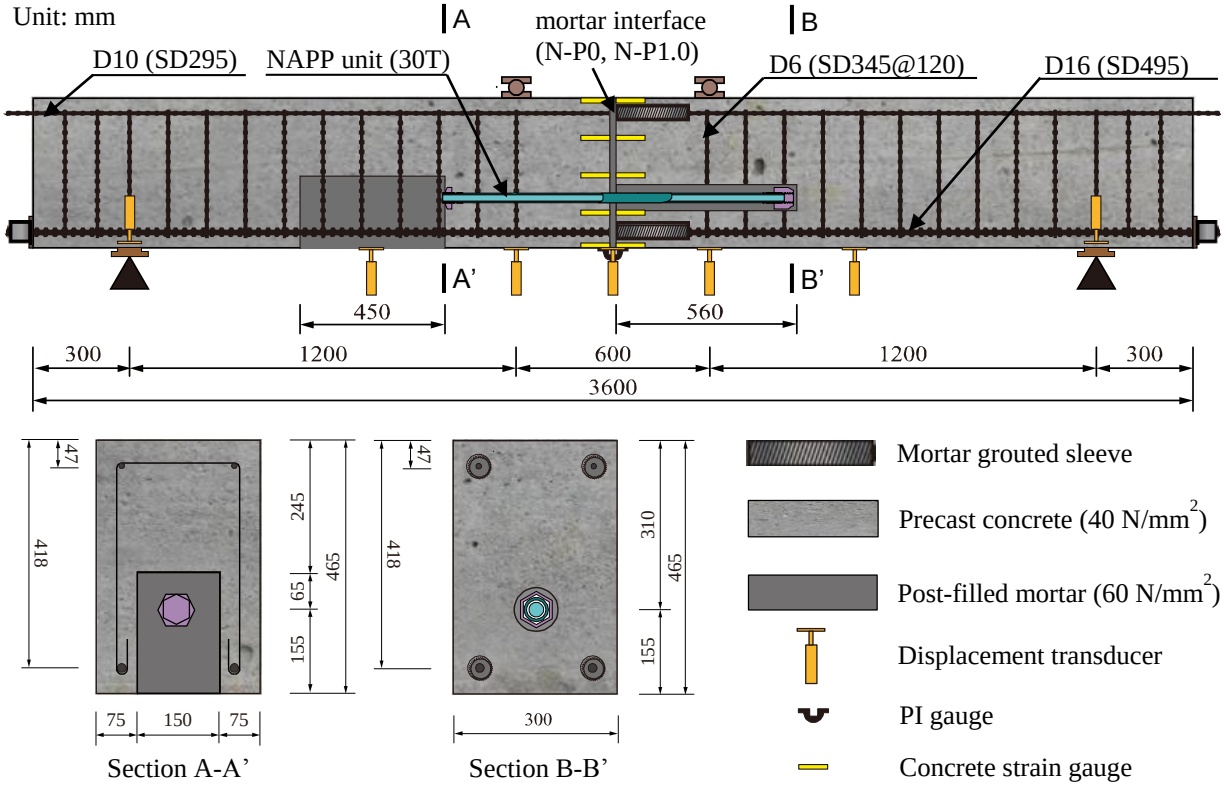

Fig. 2 Specimen dimensions and reinforcement arrangement

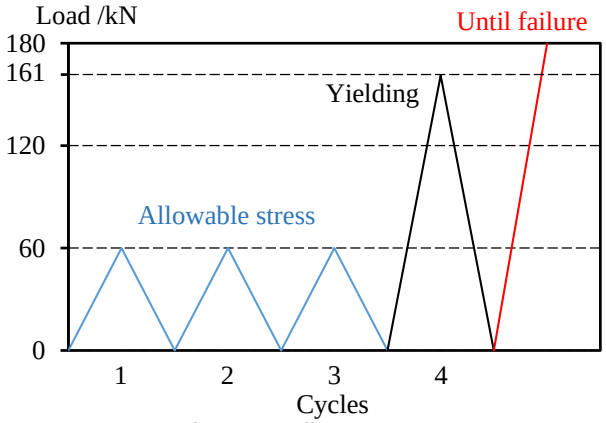

Fig. 3 Loading system

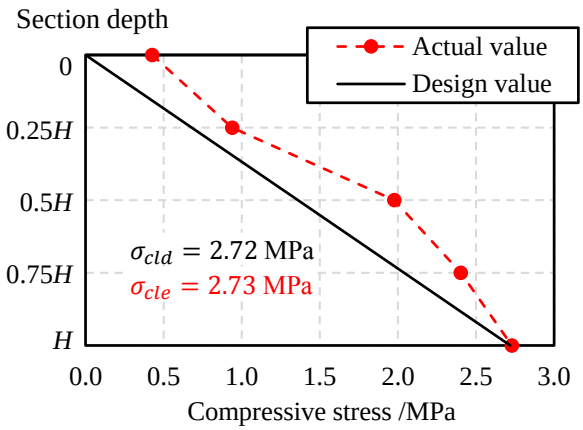

Fig. 4 Prestressing result

concrete at 5 depths (0, 116.25 mm, 232.5 mm, 348.75 mm, 465 mm from the top surface). PI gauges were attached under the interface to measure the interface opening between two PCa segments. The displacements at supports, mid-span of segments, loading points and interface were measured by transducers.

Loading system was determined as illustrated in Fig. 3. Three levels of load were considered in this study. The first level was 3 cycles of 60 kN, corresponding to the stress of 180 N/mm^2 in the tensile reinforcement, which is defined as the allowable stress of steel bars in the Specifications for Highway Bridges [5]. The second level was 1 cycle of 161 kN, which was the yielding load of tensile reinforcement calculated from nominal yielding strength. And the last level corresponded to the failure of specimens. At the peak load of 1-4 cycles, the maximum crack width was measured by a crack scale ruler.

3. EXPERIMENTAL RESULTS AND DISCUSSION

3.1 Prestressing Result

Compressive tests on concrete cylinders were conducted to obtain the actual elastic modulus of all specimens in this study. The compressive stress in concrete at the interface between PCa segments caused by prestressing was calculated by multiplying the actual strain of concrete measured as mentioned above by the experimental elastic modulus shown in Table 2. The results of prestressing in N-P1.0 are illustrated in Fig. 4, where the horizontal axis represents the compressive stress in concrete and H in the vertical axis stands for the section depth.

In Fig. 4, σ_{cld} stands for the design value of compressive stress at the bottom fiber of concrete and σ_{cle} denotes the actual value measured at 48 hours after the releasing of NAPP unit. It is shown that the requirement for prestressing force in this study was well fulfilled by using NAPP method.

3.2 Load-deflection Curves

Load-deflection curves are depicted in Fig. 5 and Table 2 summarizes the calculated values using actual strengths of materials and experimental values of yielding load and flexural capacity of all specimens. The calculation of yielding load and flexural capacity followed the stipulations in JSCE Standard Specification [4], based on the plane section hypothesis. The deflection in Fig. 5 referred to the deflection at the interface between PCa segments, namely mid-span of the specimen. The experimental yielding load $P_{y\text{-}exp}$ was obtained from the load-deflection curve where the slope dropped significantly just after the elastic stage.

Table 2 shows that the yielding load and flexural capacity of PCa beams connected by mortar grouted sleeves with prestressing force at the interface can be accurately predicted by JSCE Standard Specification with difference less than 10%. While conservative results of flexural capacity were obtained, yielding load was slightly overestimated. From the table, it can be also concluded that the existence of interface in PCa beams did not decrease the yielding load and flexural capacity compared with the monolithic beam. And prestressing force has no significant effects on them either.

Nevertheless, the whole loading processes were not exactly same in three specimens, which can be reflected from Fig. 5. In spite of the similarity in yielding load and flexural capacity, the ductility of N-P1.0 was significantly improved, indicated by more sustained duration of yielding stage than that of N-Ref and N-P0. Moreover, N-P0 was less ductile than N-Ref, where the load dropped suddenly after the peak point.

Another conclusion that can be drawn from Fig. 5 is that while the deflection of PCa beam N-P0 was larger than that of the monolithic beam N-Ref, prestressing force significantly improved the stiffness of PCa beam N-P1.0. The improvement can be clearly reflected from Fig. 5 (b) and the deflection distribution shown in Fig. 6 as well.

3.3 Interface Opening

As mentioned above, PI gauges were attached at the bottom surface of concrete to capture the interface opening of the specimens during loading tests. The results are illustrated in Fig. 7. It can be concluded that prestressing force effectively improved the resistance against the interface opening in PCa beams for the interface opening values in N-P1.0 was approximately 10% of that in N-P0 during first three cycles of loading and 66% at the yielding load. Besides, joints in both specimens were proved to be stable, indicated by insignificant increment in the interface opening values as

Table 2 Summary of experimental results

Specimen	f_y (N/mm²)	f'_c (N/mm²)	E_c (kN/mm²)	Yielding load			Flexural capacity		
				P_{y_cal} (kN)	P_{y_exp} (kN)	P_{y_exp}/P_{y_cal}	P_{u_cal} (kN)	P_{u_exp} (kN)	P_{u_exp}/P_{y_cal}
N-Ref	546	41.3	24.7	179.2	169.2	0.95	186.2	193.4	1.04
N-P0		38.7	26.3	178.8	168.5	0.94	185.8	201.8	1.09
N-P1.0		40.7	30.8	179.1	170.1	0.95	186.1	195.6	1.05

f_y: actual yield strength of tensile reinforcement, f_c': actual compressive strength of concrete, E_c: experimental value of elastic modulus, P_{y_cal}: calculated value of yielding load using actual strengths, P_{y_exp}: experimental value of yielding load, P_{u_cal}: calculated value of flexural capacity using actual strengths, P_{u_exp}: experimental value of flexural capacity

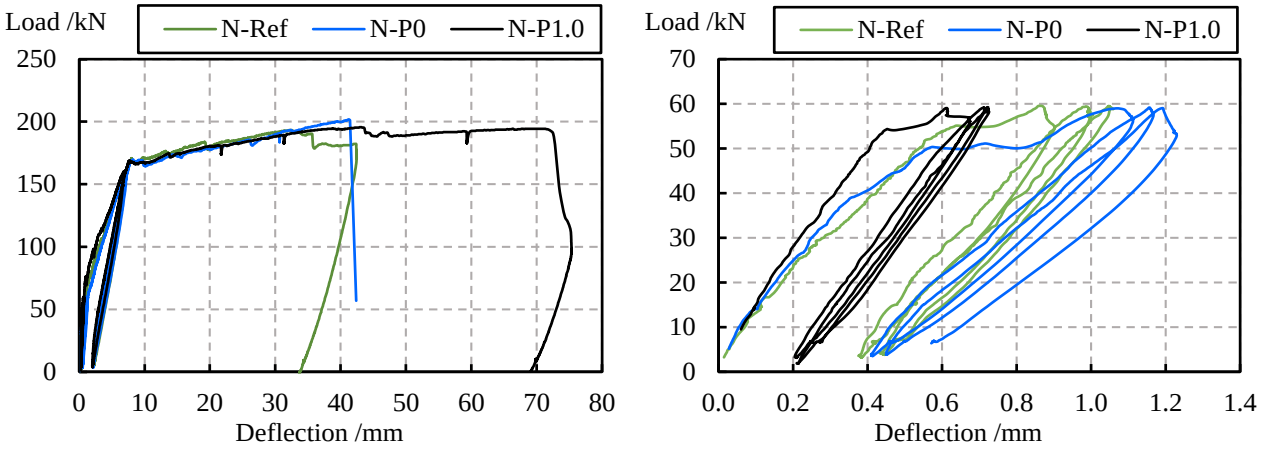

(a) Whole process of loading test (b) First 3 cycles of loading test (0~60 kN)

Fig. 5 Load-deflection curves

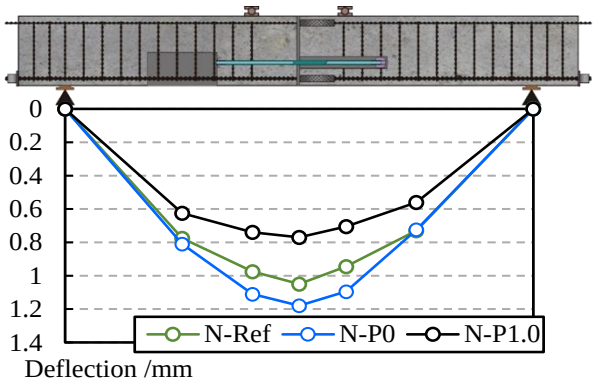

Fig. 6 Deflection distribution at 3rd cycle (60 kN)

the cyclic loading proceeded.

3.4 Crack Patterns

The initial cracking loads of all specimens were summarized in Table 3, where the cracking load of N-P1.0 was 10 kN higher than that of N-P0. After first 3 cycles of loading, cracks already appeared in the area with NAPP unit (NAPP area) in N-P0 and N-Ref while in N-P1.0, the first crack appeared outside NAPP area and no cracks appeared in NAPP area until 112 kN. Figure 8 shows crack patterns of all specimens after first three cycles of loading. It can be seen that the number of cracks in N-P1.0 was much smaller than that in N-P0. And the cracks in N-P1.0 were even fewer than that in N-Ref, from which it can be concluded that prestressing force significantly improved cracking resistance of concrete in PCa beams.

As mentioned above, the maximum crack width of each specimen was measured by a crack scale ruler at the peak load of 1-4 cycles during the loading test. Table 4 summarizes the results of 3rd and 4th cycle, and shows the comparison between experimental values and calculated values using Eq. 2 from JSCE Standard Specification [4].

$$w = 1.1k_1k_2k_3\{4c + 0.7(c_s - \phi)\}\left[\frac{\sigma_{se}}{E_s} + \varepsilon'_{csd}\right] \quad (2)$$

where, w: crack width (mm), k_1: coefficient regarding surface geometry of reinforcement, k_2: coefficient regarding concrete quality, k_3: coefficient regarding multiple layers of tensile reinforcement, c: depth of concrete cover (mm), c_s: center-to-center spacing of tensile reinforcements (mm), ϕ: diameter of tensile reinforcement (mm), σ_{se}: increment of stress in reinforcement (N/mm²), E_s: elastic modulus of reinforcement (N/mm²), ε'_{csd}: compressive strain regarding additional increment in crack width caused by shrinkage and creep of concrete.

Table 4 shows that calculated crack widths using

Table 3 Summary of initial cracking load

	N-Ref	N-P0	N-P1.0
Initial cracking load (kN)	56	45	55

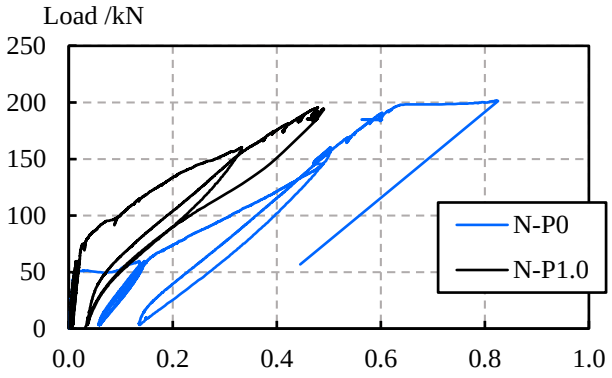

(a) Whole process of loading test

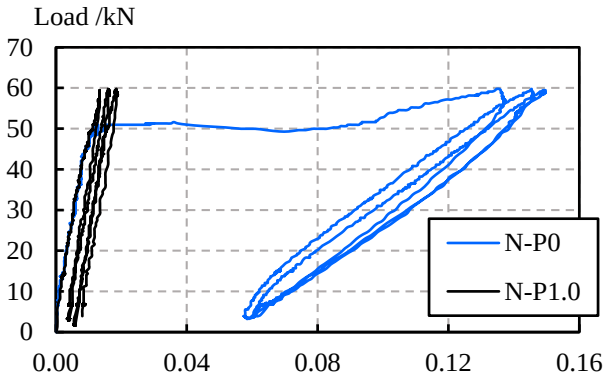

(b) First 3 cycles of loading test (0~60 kN)

Fig. 7 Load-interface opening curves

Eq. 2 were in relatively good agreement with the experimental values with the difference of around 20% at the peak load of 3rd cycle in the loading test. However, the difference became larger and more deviated at 4th cycle. This indicates that the equation for calculating crack width in RC members suggested by JSCE Standard Specification can be also applicable in PCa beams. But the results are conservative and more accurate only when the stress in tensile reinforcement is not so high and does not reach the yielding point.

In terms of relationship between crack width and interface opening, Table 4 shows that experimental values of crack width and interface opening in N-P0 were nearly same but the situation became different in N-P1.0. At the 3rd cycle of loading test, the interface opening was only about 29% of the maximum crack width while at the 4th cycle, it grew to be 132% of the maximum crack width. This may indicate that although prestressing force can effectively improve cracking resistance as well as reduce the interface opening in PCa beams, the effect on cracking resistance is more significant than that on interface opening when the load is high and the stress in tensile reinforcement gets close to the yielding point.

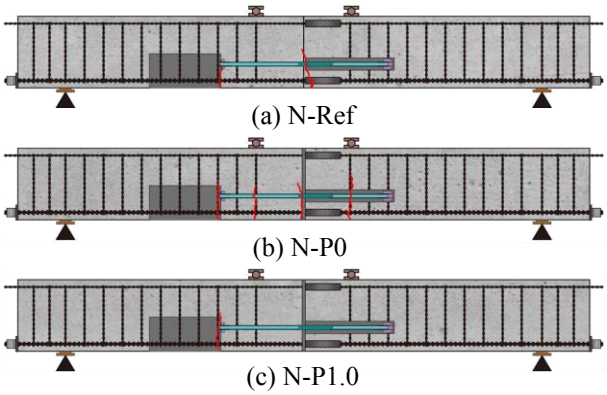

(a) N-Ref

(b) N-P0

(c) N-P1.0

Fig. 8 Crack patterns at 3rd cycle (60 kN)

3.5 Failure Mode

Crack patterns of all specimens at failure are shown in Fig. 9. Failures happened just outside NAPP area in all specimens, which was exactly as expected. In theory, the reinforcement ratio drops abruptly at two ends of NAPP unit whereas the flexural moment barely changed at the section. Cracks mainly ran vertically in all specimens and propagated at the top heading for the loading points, which showed characteristics of flexural shear cracks. Crushed concrete near the top of beams was found in all specimens despite that N-Ref failed in the right hand side while N-P0 and N-P1.0 failed in the left hand side with concrete spalling at the bottom area near the interface between the perforated hole and PCa concrete, as shown in Fig. 9. On the contrary, there was no macroscopic damage near the interface between the PCa segments both in N-P0 and N-P1.0. Figure 10 shows the damage state near the perforated hole and the interface at failure in N-P1.0. However, in this study, no causal relationship between the perforated hole and the failure of a specimen was proved for, as mentioned above, N-Ref did not fail at the side with the perforated hole. And by applying prestressing force, the cracking resistance and interface opening resistance of PCa beams were evidently improved although the new interface appeared. Therefore, it is still considered to be of certain application values to apply prestressing method in PCa structures by using NAPP method and, as this study is the first attempt, further researches are necessary for

Table 4 Summary of crack width and interface opening

Specimen	3rd cycle (60 kN)					4th cycle (161 kN)				
	w_{exp} (mm)	w_{cal} (mm)	w_{exp} / w_{cal}	w_{int} (mm)	w_{int} / w_{exp}	w_{exp} (mm)	w_{cal} (mm)	w_{exp} / w_{cal}	w_{int} (mm)	w_{int} / w_{exp}
N-Ref	0.15	0.20	0.75	-	-	0.60	0.55	1.10	-	-
N-P0	0.15	0.21	0.72	0.15	0.99	0.55	0.62	0.89	0.50	0.91
N-P1.0	0.07	0.08	0.85	0.02	0.29	0.25	0.44	0.57	0.33	1.32

w_{exp}: experimental value of maximum crack width, w_{cal}: calculated value of maximum crack width, w_{int}: experimental value of interface opening

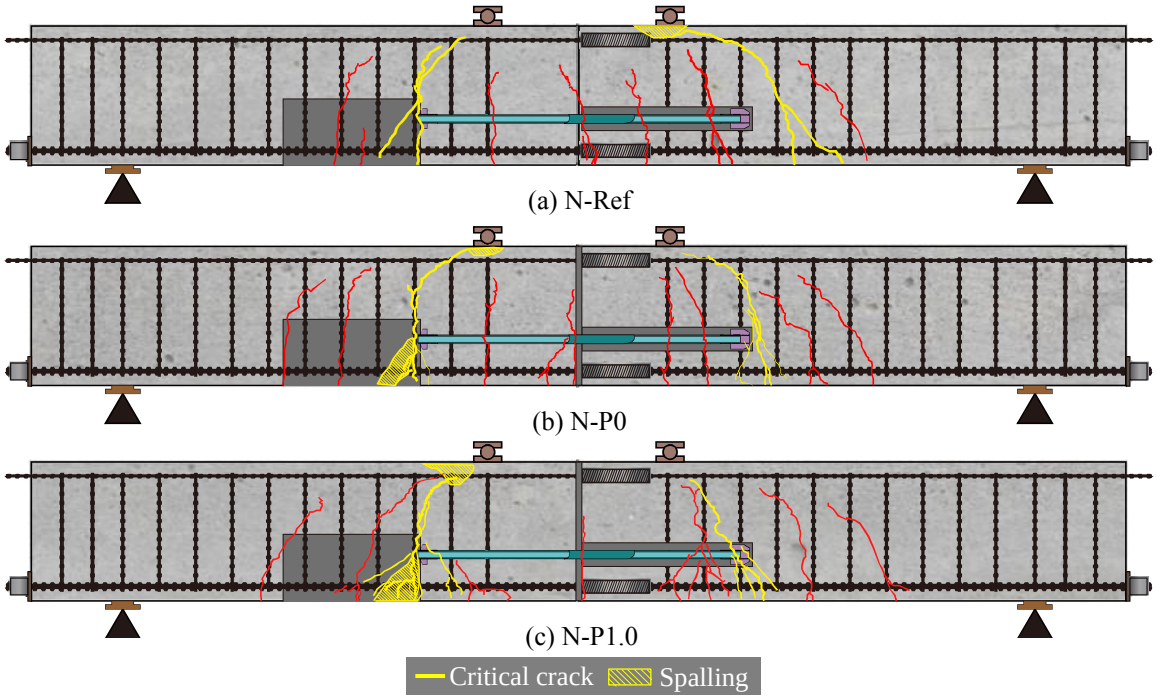

Fig. 9 Crack patterns at failure

(a) Perforated hole (b) Interface

Fig. 10 Damage state in N-P1.0

more improvements on this engineering method.

4. CONCLUSIONS

Based on the experimental results of loading tests on three beam specimens considering the prestressing force at the interface between PCa segments, the following conclusions can be deduced in this study:

(1) The requirement for design prestressing force used to connect PCa segments can be fulfilled by using NAPP method.

(2) The existence of interface and prestressing force do not have significant effects on the yielding load and ultimate flexural capacity of PCa beams. Although the ductility of PCa beams was decreased compared with monolithic RC beams, prestressing method can offset the decrease and provide even better ductility to PCa beams than monolithic RC beams.

(3) Prestressing method can effectively reduce the deflection as well as interface opening and significantly improve the cracking resistance in PCa beams.

(4) The equation for estimating crack width in RC members suggested by JSCE Standard Specification can be also applied in PCa beams. But it is reliable only when the stress in tensile reinforcement does not reach the yielding point.

(5) Although a new interface appears between the perforated hole and PCa concrete where the failure is likely to happen, it is still of application values to apply prestressing method in PCa structures by using NAPP method.

ACKNOWLEDGEMENT

This research has been supported by JSPS Grant-in-Aid for Scientific Research (B), Grant Number 17H03296. The authors also sincerely acknowledge the supports from Neturen Co., Ltd. for the supply of experiment material and guidance on NAPP method.

REFERENCES

[1] Wang, H. et al., “Flexural Performance of RC Beams with Interface and Various Connections,” Proceedings of the Japan Concrete Institute, Vol. 39, No.2, 2017, pp. 421-426.

[2] Patipong, T., “Flexural Behavior of RC Beams with Connection Using Mortar Grouted Sleeves,” Master-thesis, Department of Civil Engineering, Tokyo Institute of Technology, Tokyo, 2017.

[3] NAPP Method Technological Society, “Construction and Design Manual of NAPP Anchoring Method,” 2014.

[4] JSCE, “Standard Specifications for Concrete Structures -2017, Design,” 2017.

[5] Japan Road Association, “Specifications for Highway Bridges (I Common ·III Bridges),” 2012.